VIETNAM NATIONAL UNIVERSITY HO CHI MINH CITY
HO CHI MINH CITY UNIVERSITY OF TECHNOLOGY

VIET NAM NATIONAL UNIVERSITY HO CHI MINH CITY

The 7th International Conference on Green Technology and Sustainable Development
(7th GSTD2024)
25-26 July; Ho Chi Minh city, Vietnam

Presentation – ID317:

Coordinated Control of Three-Level T-Type Inverter for Renewable Energy Applications: Integrating Predictive Control with External RLC Estimation

Tin Lu Trung[1], Khoa Dang Tran Nguyen[1], Trinh Thi Ly[1], Trang Dang Quang Pham[1], Nhuan An Le[1], Minh Duc Pham[1]

Speaker: Tin Lu Trung

(email: tin.luhcmut2003@hcmut.edu.vn)

[1] Power Electronics Research Laboratory, Ho Chi Minh city University of Technology, VNUHCM

TABLE OF CONTENTS

What is renewable energy?

Introduction

- Renewable energy is energy derived from natural sources that replenish faster than they are used.
- Sunlight and wind are prime examples of these constantly renewing sources. These renewable energy sources are abundant and readily available all around us.

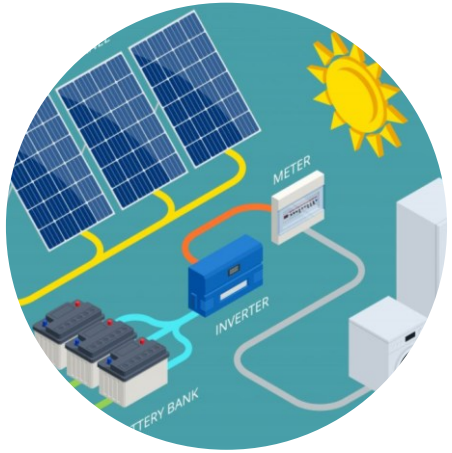

Solar Energy

Wind Energy

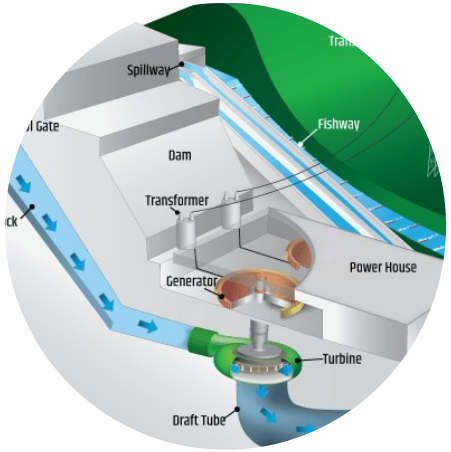

Hydropower

Hydropower

Figure 1. Example of renewable energy sources

Introduction

- In the field of renewable energy, three-phase inverters play a crucial role to convert DC voltage to AC voltage.

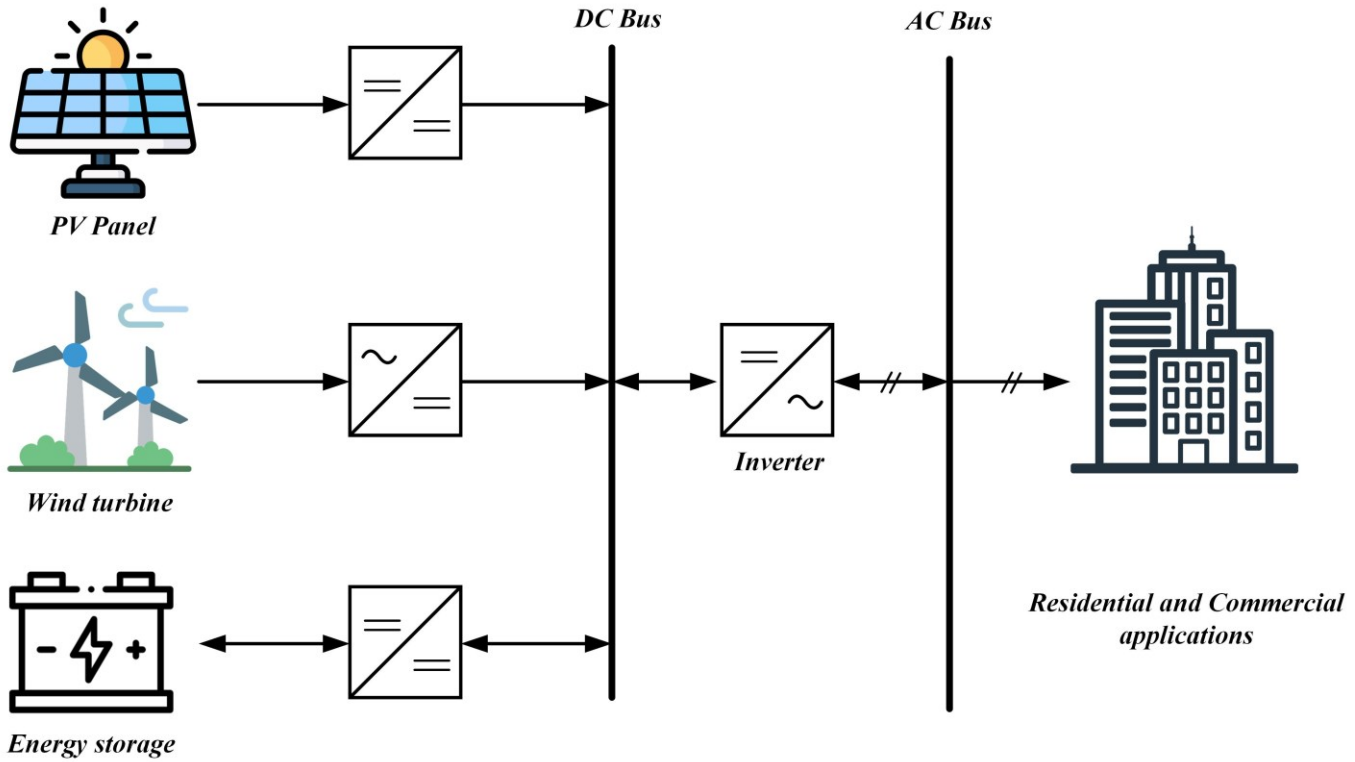

Figure 2. Role of inverter in renewable energy

Introduction

- However, today's most popular inverter types are the 2-level inverter and the 3-level diode-clamped inverter (3L-DCI). Despite their popularity, these inverters have significant disadvantages, including high switching losses and poor total harmonic distortion (THD).
- To improve the above shortcomings, researchers proposed a new topology for the inverter, the T-Type 3-level inverter.

Introduction

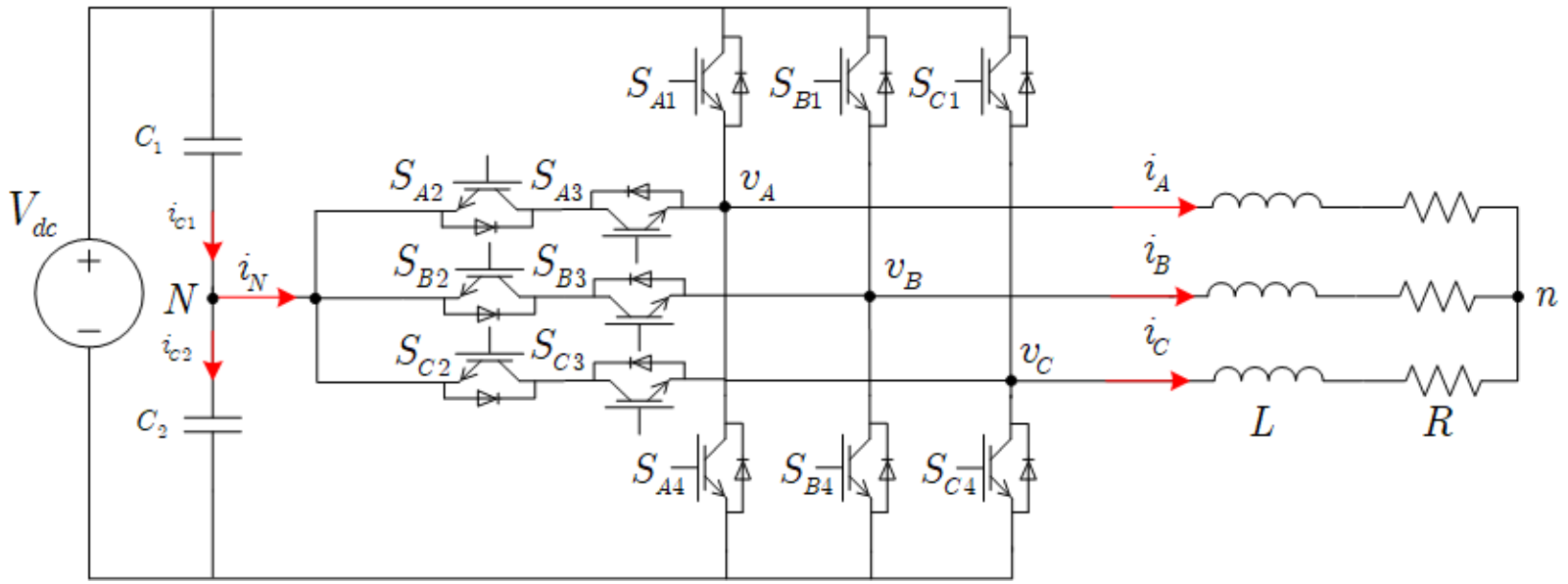

Figure 3. T-Type Three Level Inverter Typology.

Introduction

- However, this configuration can lead to a neutral-point voltage imbalance, resulting in increased harmonic distortion.
- To address this, **current control methods** for T-type inverter circuits have been proposed.
- The authors Nachiappan proposed a proportional-integral (PI) current controller with pulse width modulation in [6].

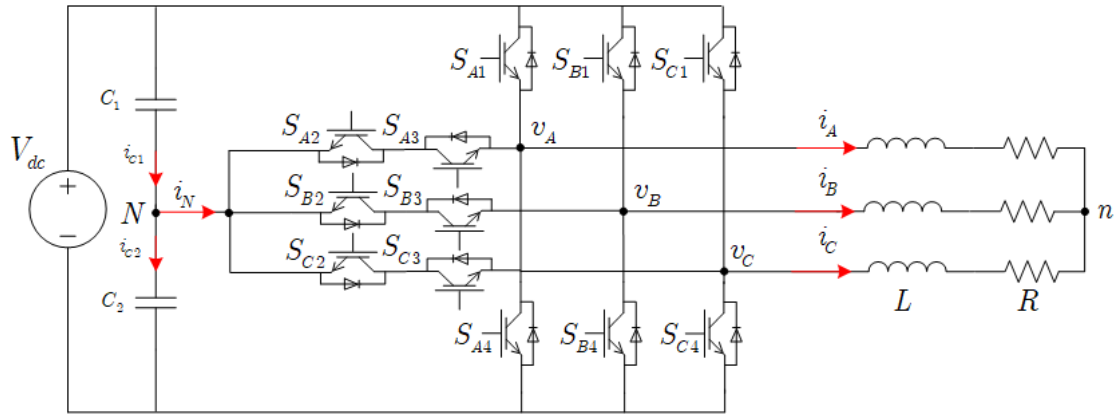

Figure 3. T-Type Three Level Inverter Typology.

Introduction

- With the advancement of microprocessors, there has been extensive research into predictive control solutions for power converters.
- In [7], Xu proposed a modulated model predictive control and compared it with the conventional PI Controller to highlight the effectiveness of predictive control.
- However, limited research has been conducted on coordinating the current MPC control scheme with an **external RLC online estimator.**

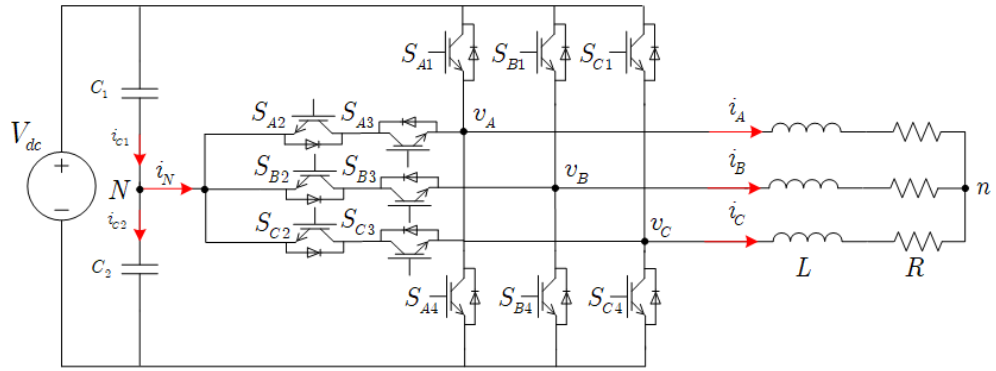

Figure 3. T-Type Three Level Inverter Typology.

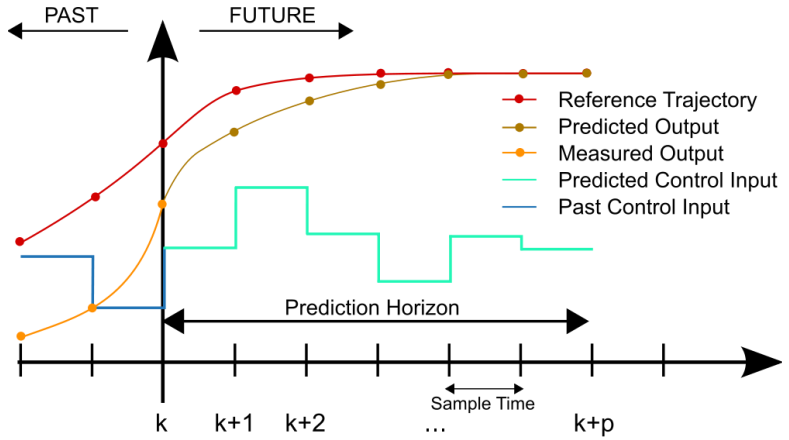

Figure 4. Model Predictive Control Scheme.

Introduction

- This paper presents a coordinated control approach integrating a model predictive control scheme with an extern RLC online estimator.
- The proposed strategy targets the precise tracking the output of the 3LT2I, ensuring fast response times, balanced capacitor voltage, and continuous updating of load impedance parameter data to uphold optimal current control performance.
- Simulations are conducted under various load scenarios to validate the feasibility and effectiveness of the proposed control method.

TABLE I. OUTPUT VOLTAGE OF EACH PHASE UNDER DIFFERENT SWITCHING STATES FOR THE 3LT2I INVERTER.

For Phase P *with* $P \in \{A, B, C\}$					
Switching States	***Device State***				***Output Voltage***
S_P	S_{P1}	S_{P2}	S_{P3}	S_{P4}	v_{Pn}
0	0	0	1	1	0
1	0	1	1	0	$V_{dc}/2$
2	1	1	0	0	V_{dc}

- Table I presents the switching states and output phase leg voltages of 3LT2I.
- The phase leg voltage can be derived as follows:

$$v_{Pn} = S_P \frac{V_{dc}}{2}$$

Modelling of T-type Three-level Inverter

- The output voltage of 3LT2I is the inverter voltage vector, the space voltage of the inverter needs to be converted to $\alpha\beta$ coordination for easier presentation and analysis.

$$\vec{v}_{\alpha\beta} = \frac{2}{3}\left(v_{An} + e^{j2\pi/3}v_{Bn} + e^{j4\pi/3}v_{Cn}\right)$$

- Similarly, the output current in $\alpha\beta$ frame is determined as follows:

$$\vec{i}_{\alpha\beta} = \frac{2}{3}\left(i_A + e^{j2\pi/3}i_B + e^{j4\pi/3}i_c\right)$$

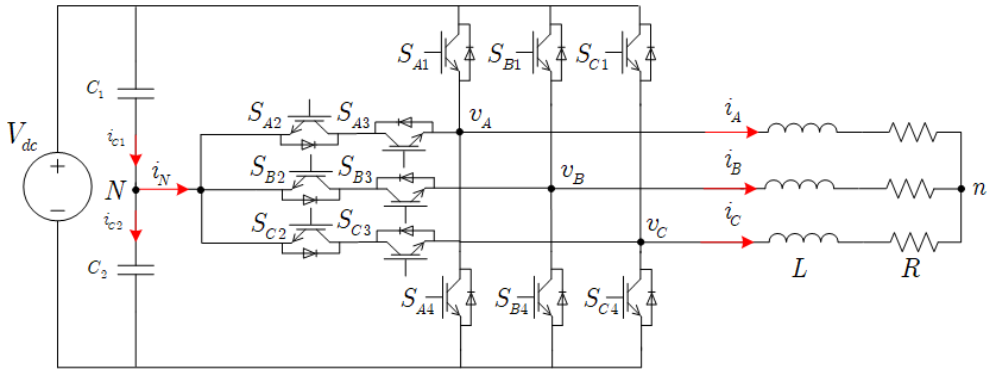

Figure 3. T-Type Three Level Inverter Typology.

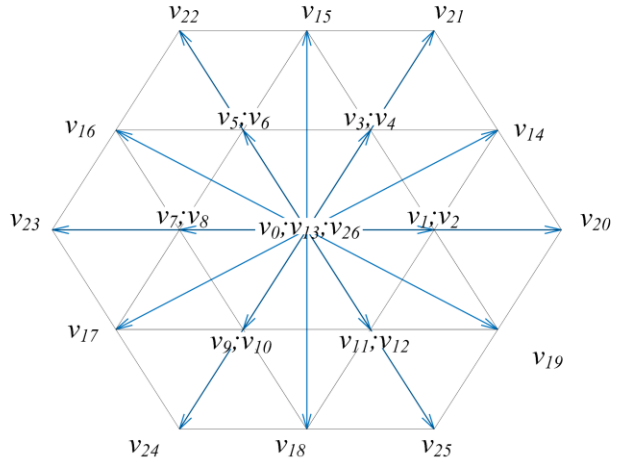

Figure 5. Representation of Space Vector for a 3-Level T-Type Inverter

TABLE II. STATES OF SWITCHING DEVICES AND VOLTAGE VECTORS

Type of voltage vector	State	Output Phase Voltages			Voltage Vector (v_k)
	$S_A S_B S_C$	*Phase A voltage* (v_{An})	*Phase B voltage* (v_{Bn})	*Phase C voltage* (v_{Cn})	
Zero	*000*	0	0	0	$v_0 = 0\angle 0°$
	222	V_{dc}	V_{dc}	V_{dc}	$v_{13} = 0\angle 0°$
	111	$V_{dc}/2$	$V_{dc}/2$	$V_{dc}/2$	$v_{26} = 0\angle 0°$
Small	*100;211*	$V_{dc}/2;V_{dc}$	$0;V_{dc}/2$	$0;V_{dc}/2$	$v_1;v_2 = V_{dc}/3\angle 0°$
	221;110	$V_{dc};V_{dc}/2$	$V_{dc};V_{dc}/2$	$V_{dc}/2;0$	$v_3;v_4 = V_{dc}/3\angle 60°$
	121;110	$V_{dc}/2;0$	$V_{dc};V_{dc}/2$	$V_{dc}/2;0$	$v_5;v_6 = V_{dc}/3\angle 120°$
	122;011	$V_{dc}/2;0$	$V_{dc};V_{dc}/2$	$V_{dc};V_{dc}/2$	$v_7;v_8 = V_{dc}/3\angle 180°$
	001;112	$0;V_{dc}/2$	$0;V_{dc}/2$	$V_{dc}/2;V_{dc}$	$v_9;v_{10} = V_{dc}/3\angle 240°$
	101;212	$V_{dc}/2;V_{dc}$	$0;V_{dc}/2$	$V_{dc}/2;V_{dc}$	$v_{11};v_{12} = V_{dc}/3\angle 300°$
Medium	*120*	$V_{dc}/2$	V_{dc}	0	$v_{14} = \sqrt{3}V_{dc}/3\angle 30°$
	021	0	V_{dc}	$V_{dc}/2$	$v_{15} = \sqrt{3}V_{dc}/3\angle 90°$
	102	$V_{dc}/2$	0	V_{dc}	$v_{16} = \sqrt{3}V_{dc}/3\angle 150°$
	201	V_{dc}	0	$V_{dc}/2$	$v_{17} = \sqrt{3}V_{dc}/3\angle 210°$
	210	V_{dc}	$V_{dc}/2$	0	$v_{18} = \sqrt{3}V_{dc}/3\angle 270°$
	012	0	$V_{dc}/2$	V_{dc}	$v_{19} = \sqrt{3}V_{dc}/3\angle 330°$
Large	200	V_{dc}	0	0	$v_{20} = 2V_{dc}/3\angle 0°$
	220	V_{dc}	V_{dc}	0	$v_{21} = 2V_{dc}/3\angle 60°$
	020	0	V_{dc}	0	$v_{22} = 2V_{dc}/3\angle 120°$
	022	0	V_{dc}	V_{dc}	$v_{23} = 2V_{dc}/3\angle 180°$
	002	0	0	V_{dc}	$v_{24} = 2V_{dc}/3\angle 240°$
	202	V_{dc}	0	V_{dc}	$v_{25} = 2V_{dc}/3\angle 300°$

Proposed control method

- The goal of the control scheme is to accurately track the output current and maintain balance in capacitor voltage.
- This objective is achieved through the application of the finite control set – model predictive control (FCS-MPC) algorithm, which comprises a cost function with two main components: current tracking and capacitor voltage balancing.
- Additionally, the RLC online estimator periodically updates the load parameters, thereby enhancing the accuracy of the current tracking component.

Proposed control method

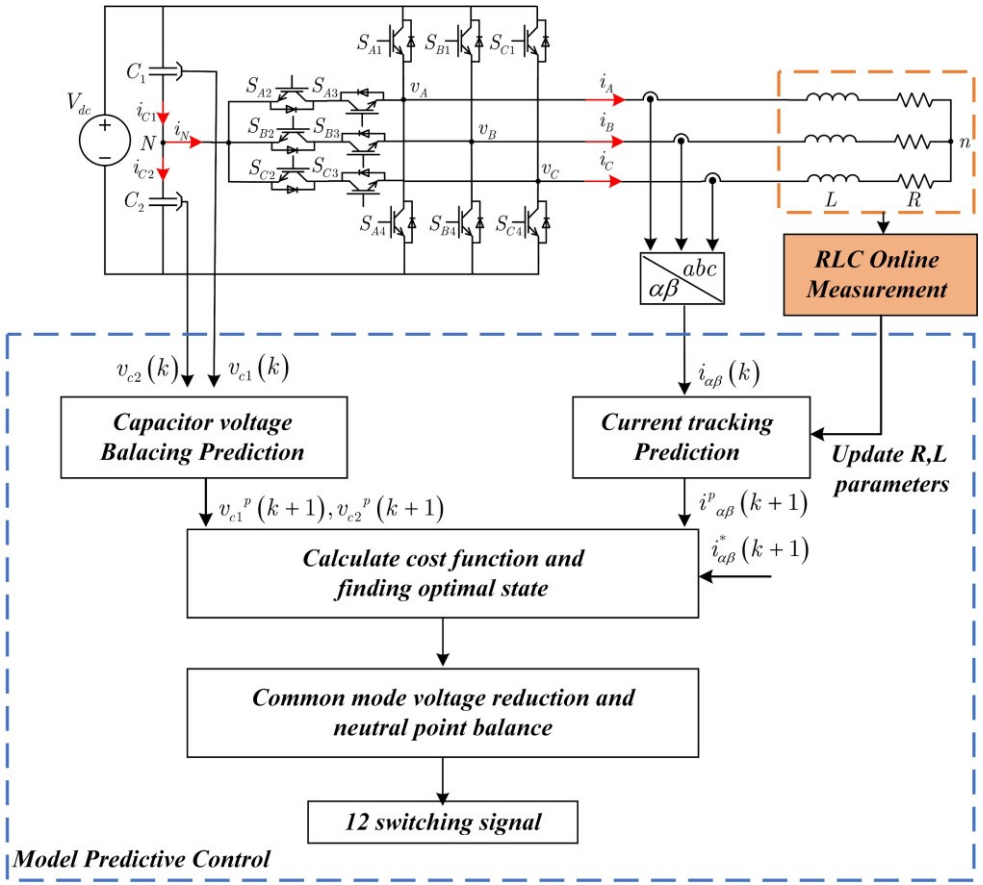

Figure 6. The block diagram of proposed Model Predictive Control

a. Predictive Current Equation and its Cost Function

- The mathematical depiction of the 3LT2I model in continuous time is outlined below:

$$\begin{cases} v_{An} = i_A R + L\dfrac{di_A}{dt} + V_{nN} \\ v_{Bn} = i_B R + L\dfrac{di_B}{dt} + V_{nN} \\ v_{Cn} = i_C R + L\dfrac{di_C}{dt} + V_{nN} \end{cases}$$

- In which V_{nN} represents the voltage between the neutral point of the load and the N point of DC bus.
- R and L are the load resistance and inductance.

Proposed control method

a. Predictive Current Equation and its Cost Function

- The system mathematical model can be then rewritten in $\alpha\beta$ coordinates as shown in the following equation:

$$v_{\alpha\beta} = i_{\alpha\beta} R + L \frac{di_{\alpha\beta}}{dt}$$

- The Euler approximation method to convert the system model from the continuous domain to the discrete domain is using the equation presented below:

$$\frac{dx}{dt} \approx \frac{x(k+1) - x(k)}{T_s}$$

- The future output current at the time $k+1$ in the discrete domain as follows:

$$i_{\alpha\beta}(k+1) = \left(1 - \frac{R}{L} T_s\right) i_{\alpha\beta}(k) + \frac{T_s}{L} v_{\alpha\beta}(k)$$

Proposed control method

a. Predictive Current Equation and its Cost Function

- The $k+1$ current caculated needs to track the reference current, which is discretized from the standard sinusoidal current.
- Hence, the cost function for current tracking is determined below:

$$J_i = \left|i_\alpha^*(k+1) - i_\alpha(k+1)\right| + \left|i_\beta^*(k+1) - i_\beta(k+1)\right|$$

b. Predictive Capacitor Voltage Equation and its Cost Function

- In Fig, 3, the current is denoted as i_N represents the neutral point current.
- This current is calculated based on the relationship between the switching states define in Table I and the three phase output current as follows:

$$i_N(k) = \left[S_{A2}(k) - S_{A1}(k)\right] i_A(k) + \left[S_{B2}(k) - S_{B1}(k)\right] i_B(k) + \left[S_{C2}(k) - S_{C1}(k)\right] i_C(k)$$

- The differential equation describing the capacitor voltages v_{c1}, v_{c2}

$$\begin{cases} \dfrac{dv_{C1}}{dt} = \dfrac{1}{2C} i_N \\ \dfrac{dv_{C2}}{dt} = -\dfrac{1}{2C} i_N \end{cases}$$

b. Predictive Capacitor Voltage Equation and its Cost Function

- The predicted capacitor voltage at the time $k+1$ is calculated as shown below:

$$\begin{cases} v_{C1}(k+1) = v_{C1}(k) + \dfrac{Ts}{2C} i_N(k) \\ v_{C2}(k+1) = v_{C1}(k) - \dfrac{Ts}{2C} i_N(k) \end{cases}$$

- The cost function J_u for balancing of the DC-link capacitor voltage is formulated as follows:

$$J_u = \left| v_{C1}(k+1) - v_{C2}(k+1) \right|$$

Proposed control method

c. Current and Capacitor Voltage Cost Function

- The total cost function comprises both J_u and J_i, to attain optimal control control efficiency, the priority of the two cost function components has to be adjusted.
- The total cost function is described as:

$$J = J_i + \lambda_u J_u$$

- Where λ_u is the weighing factor in considered for the voltage cost function priority.
- After through testing and evaluation, a coefficient of $\lambda_u = 0.01$ was determined

Proposed control method

c. Current and Capacitor Voltage Cost Function

- The flowchart of a control period is shown in Fig. 7
- These predictions are obtained by applying 27 switching states outlined in Table II.
- After determining the switching state that yields the smallest cost function, the microprocessor applies the power switches in next period.

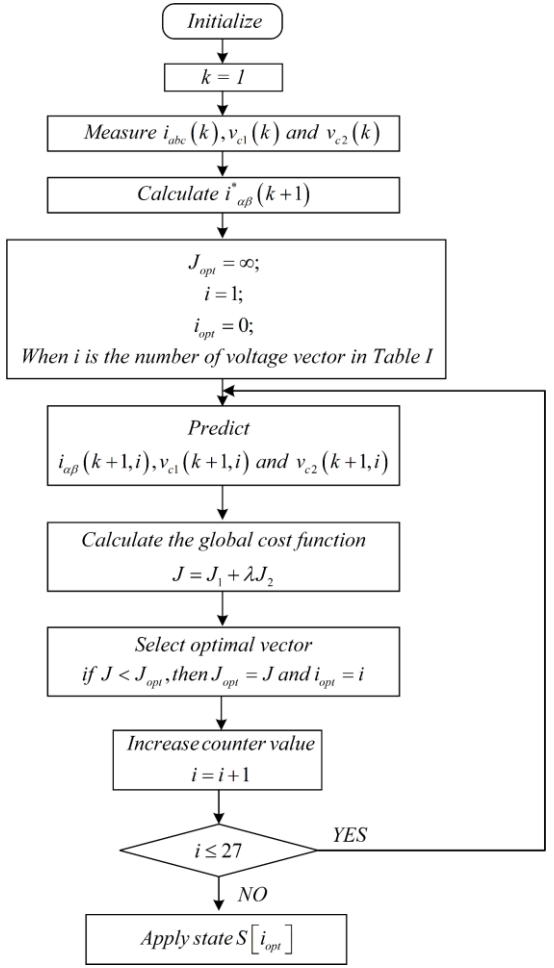

Figure 6. The flowchart of one control period

Simulation Result

- To validate the proposed control scheme, simulations were conducted.
- The first scenario focuses on analyzing the current THD and capacitor voltage when the load parameters in MPC have some mismatched value and it is divided into two states.
- The second simulation scenario assesses the current THD and capacitor voltages when the load parameters in MPC have some mismatched value and the current reference current is changed in the operation.

TABLE III. SIMULATION PARAMETERS

Parameter	Symbol	Value
DC Voltage	V_{dc}	800V
Load	R, L	25Ω,50 mH
DC-link capacitor	C_1, C_2	470 µF
Sampling frequency	f_s	10 kHz
AC Voltage Frequency	f	50 Hz
Weighting factor	λ_u	0.01

Simulation Result

A. First simulation scenario

- In stage 1, the system operates with 12.5 A current reference, the load parameters in MPC are initially $R = 25\Omega, L = 25mH$
- At the time $t = 0.05s$, State 2 starts, and the RLC online estimator updates the load parameter with right value to the current tracking prediction in the MPC

Simulation Result

A. *First simulation scenario*

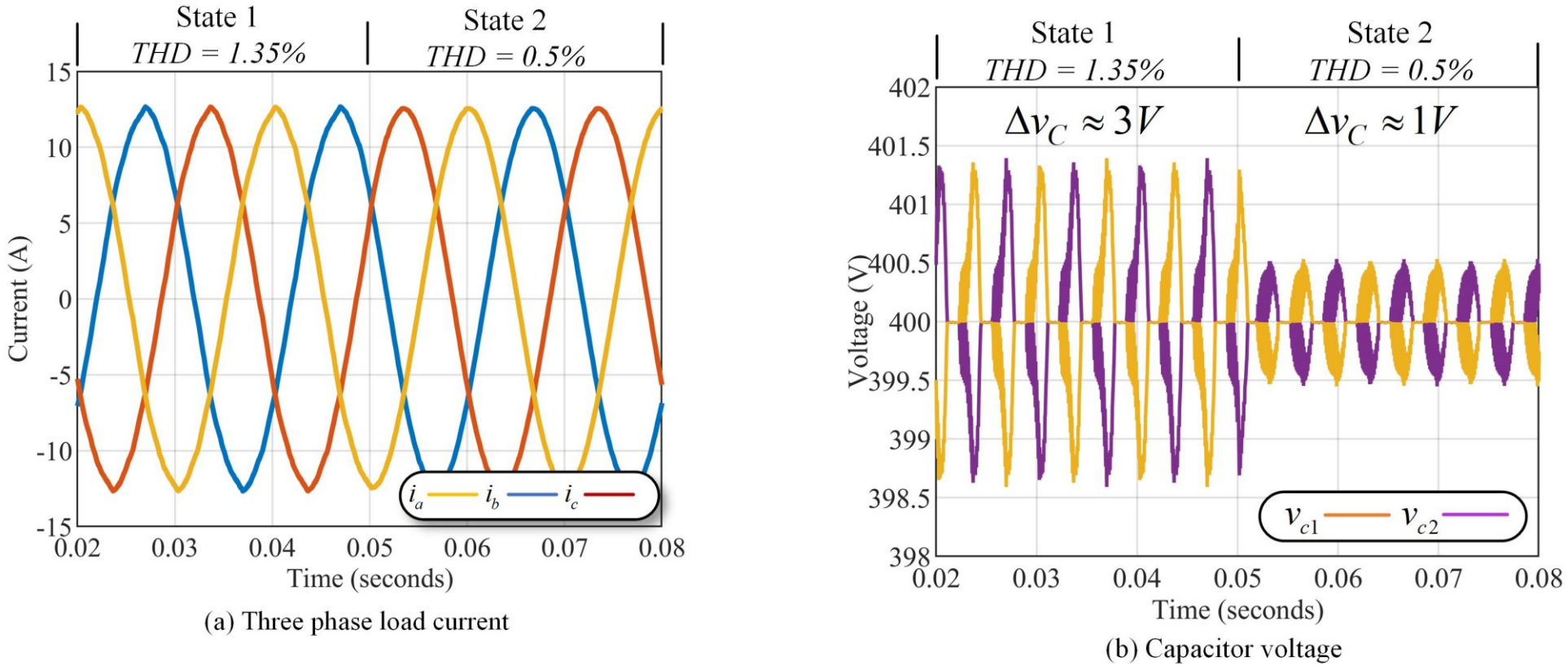

(a) Three phase load current

(b) Capacitor voltage

Figure 7. Response of 3LT2I using MPC Algorithm in the first scenario

B. Second simulation scenario

- In stage 3 the load parameters in MPC are initially $R = 25\Omega, L = 25mH$.
- At the time $t = 0.04s$, State 4 starts, and the RLC online estimator updates the load parameter with right value to the current tracking prediction in the MPC
- At the time $t = 0.09s$, the current reference is changed from 13A to 12A to validate the dynamic response of controller

Simulation Result

B. Second simulation scenario

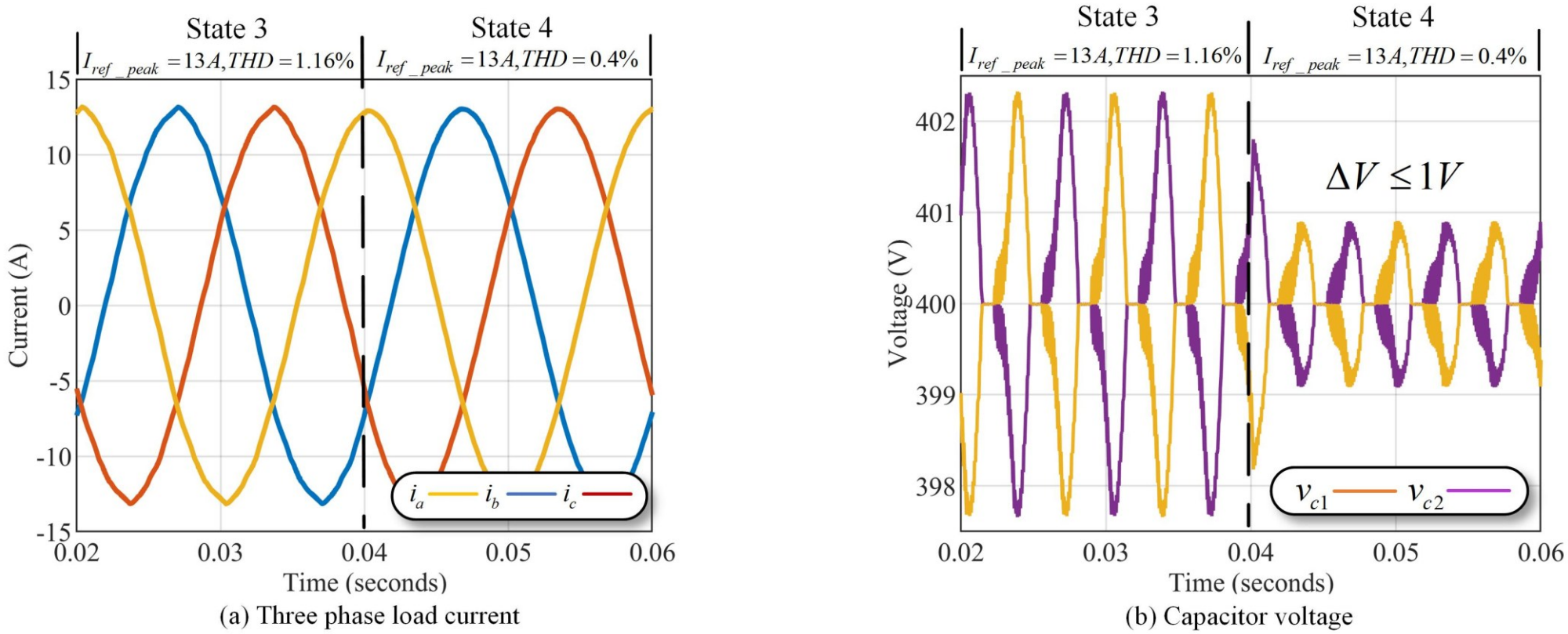

Figure 8. Response of 3LT2I using MPC Algorithm in the second scenario

Simulation Result

B. Second simulation scenario

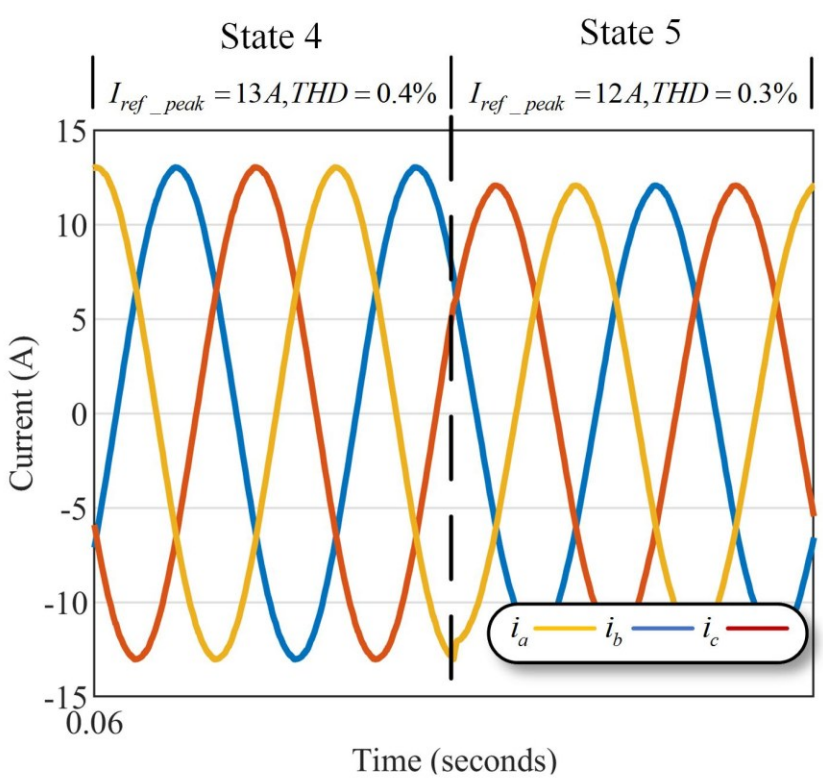

(a) Three phase load current

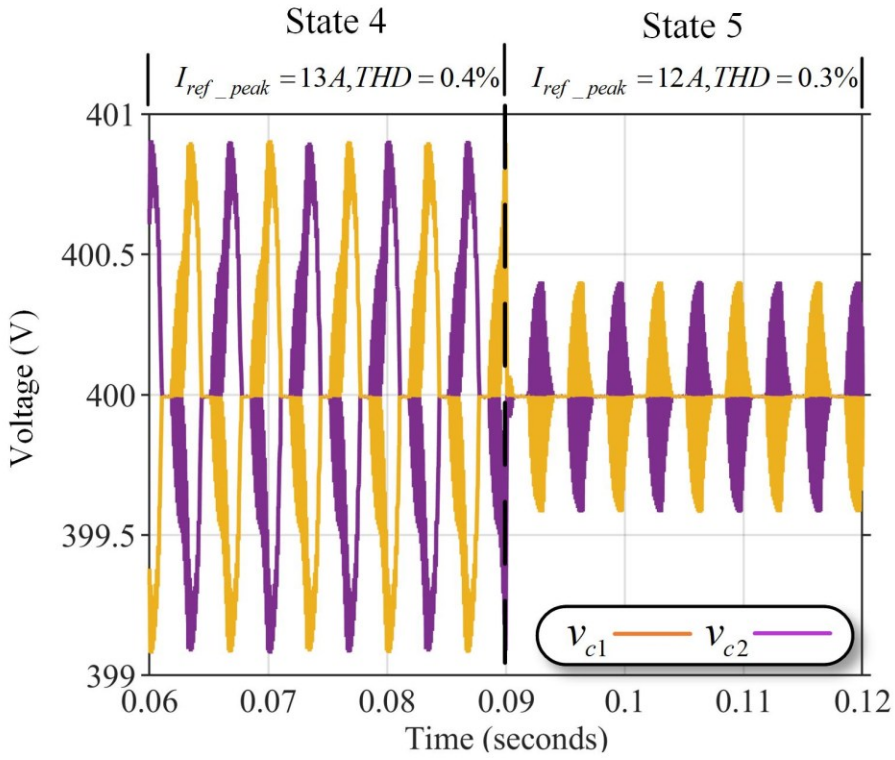

(b) Capacitor voltage

Figure 9. Response of 3LT2I using MPC Algorithm in the third scenario

Conclusion

- The integration of Model Predictive Control (MPC) with an external RLC online estimator proposed in this paper presents a coordinated control approach for achieving precise current tracking and balanced capacitor voltages in the 3LT2I system.
- The three simulation scenarios emphasized the important of properly updated load parameters and demonstrated the adaptability of the proposed control scheme to changes in current reference value, leading to a reduction in total harmonic distortion (THD) smaller than 1.5%

Reference

[1] Calif. IEEE Applied Power Electronics Conference and Exposition 31. 2016 Long Beach *et al.*, *APEC 2016 thirty first Annual IEEE Applied Power Electronics Conference and Exposition : March 20-24, 2016, Long Beach Convention Center - Long Beach, California*. IEEE, 2016.

[2] E. A. Kumar, K. C. Sekhar, and R. S. Rao, "Model Predictive Current Control of a Three-Phase T-Type NPC Inverter to Reduce Common Mode Voltage," *Journal of Circuits, Systems and Computers*, vol. 27, no. 2, Feb. 2018, doi: 10.1142/S0218126618500287.

[3] S. Kouro, P. Cortés, R. Vargas, U. Ammann, and J. Rodríguez, "Model predictive control - A simple and powerful Method to control power converters," *IEEE Transactions on Industrial Electronics*, vol. 56, no. 6, pp. 1826–1838, 2009, doi: 10.1109/TIE.2008.2008349.

[4] G. Yang, S. Hao, C. Fu, and Z. Chen, "Model Predictive Direct Power Control Based on Improved T-Type Grid-Connected Inverter," *IEEE J Emerg Sel Top Power Electron*, vol. 7, no. 1, pp. 252–260, Mar. 2019, doi: 10.1109/JESTPE.2018.2871113.

[5] Y. Liu, X. Mao, G. Ning, H. Dan, H. Wang, and M. Su, "Model Predictive-Based Voltage Balancing Control for Single-Phase Three-Level Inverters," *IEEE Trans Power Electron*, vol. 36, no. 11, pp. 12177–12182, Nov. 2021, doi: 10.1109/TPEL.2021.3077011.

[6] A. Nachiappan, K. Sundararajan, and V. Malarselvam, "Current controlled voltage source inverter using Hysteresis controller and PI controller," in *2012 International Conference on Power, Signals, Controls and Computation*, 2012, pp. 1–6.

[7] J. Xu, T. B. Soeiro, F. Gao, H. Tang, and P. Bauer, "A simplified modulated model predictive control for a grid-tied three-level T-type inverter," in *2020 IEEE 29th International Symposium on Industrial Electronics (ISIE)*, 2020, pp. 618–623.

[8] X. Wang *et al.*, "Model predictive control methods of leakage current elimination for a three-level T-type transformerless PV inverter," *IET Power Electronics*, vol. 11, no. 8, pp. 1492–1498, 2018.

[9] V.-Q.-B. Ngo, M.-K. Nguyen, T.-T. Tran, Y.-C. Lim, and J.-H. Choi, "A simplified model predictive control for T-type inverter with output LC filter," *Energies (Basel)*, vol. 12, no. 1, p. 31, 2018.

[10] N. X. Doan and N. Van Nguyen, "Improved Model Predictive Control for Asymmetric T-Type NPC 3-Level Inverter," *Electronics (Basel)*, vol. 10, no. 18, p. 2244, 2021.

[11] M. Schwenzer, M. Ay, T. Bergs, and D. Abel, "Review on model predictive control: An engineering perspective," *The International Journal of Advanced Manufacturing Technology*, vol. 117, no. 5, pp. 1327–1349, 2021.

THANKS FOR YOUR ATTENTION!